Supplementary Information

Multifunctional, Superhydrophobic and Highly Elastic MXene/Bacterial Cellulose Hybrid Aerogels Enabled via Silylation

*Daqiang Zhao[1], Le-Yang Dang[1], Gui-Gen Wang[1,] *, Na Sun[1], Xianyu Deng[1], Jie-Cai Han [3], Jia-Qi Zhu[3,]*, Ya Yang[2,]**

[1] Shenzhen Key Laboratory for Advanced Materials, School of Materials Science and Engineering, Harbin Institute of Technology (Shenzhen), Shenzhen 518055, P. R. China.

[2] CAS Center for Excellence in Nanoscience, Beijing Key Laboratory of Micro-nano Energy and Sensor, Beijing Institute of Nanoenergy and Nanosystems, Chinese Academy of Sciences, Beijing 101400, P. R. China.

[3] National Key Laboratory of Science and Technology on Advanced Composites in Special Environments, Harbin Institute of Technology, Harbin 150080, P. R. China.

*Corresponding Authors: G.-G. Wang (wangguigen@hit.edu.cn), J.Q. Zhu (zhujq@hit.edu.cn), Y. Yang (yayang@binn.cas.cn)

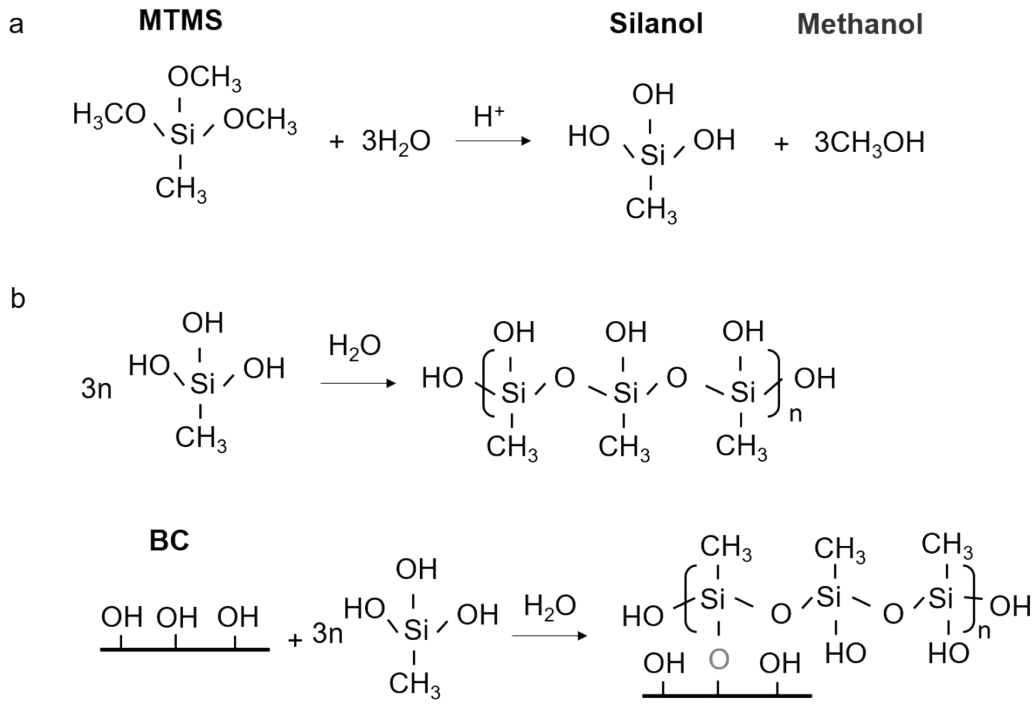

Figure S1. Schematic illustration of the reaction of MTMS in aqueous BC suspension. (a) Chemical reaction between MTMS and H_2O. (b) self-polymerization among unreacted silanols and *in situ* polymerization between unreacted silanols and hydroxyl groups.

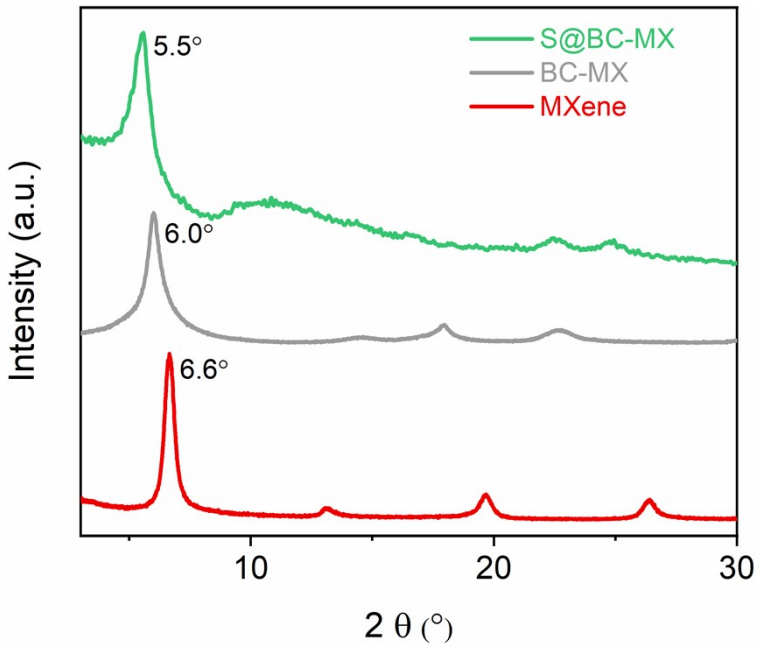

Figure S2. XRD patterns of pure MXene, BC-MX50%, and S@BC-MX50% aerogels.

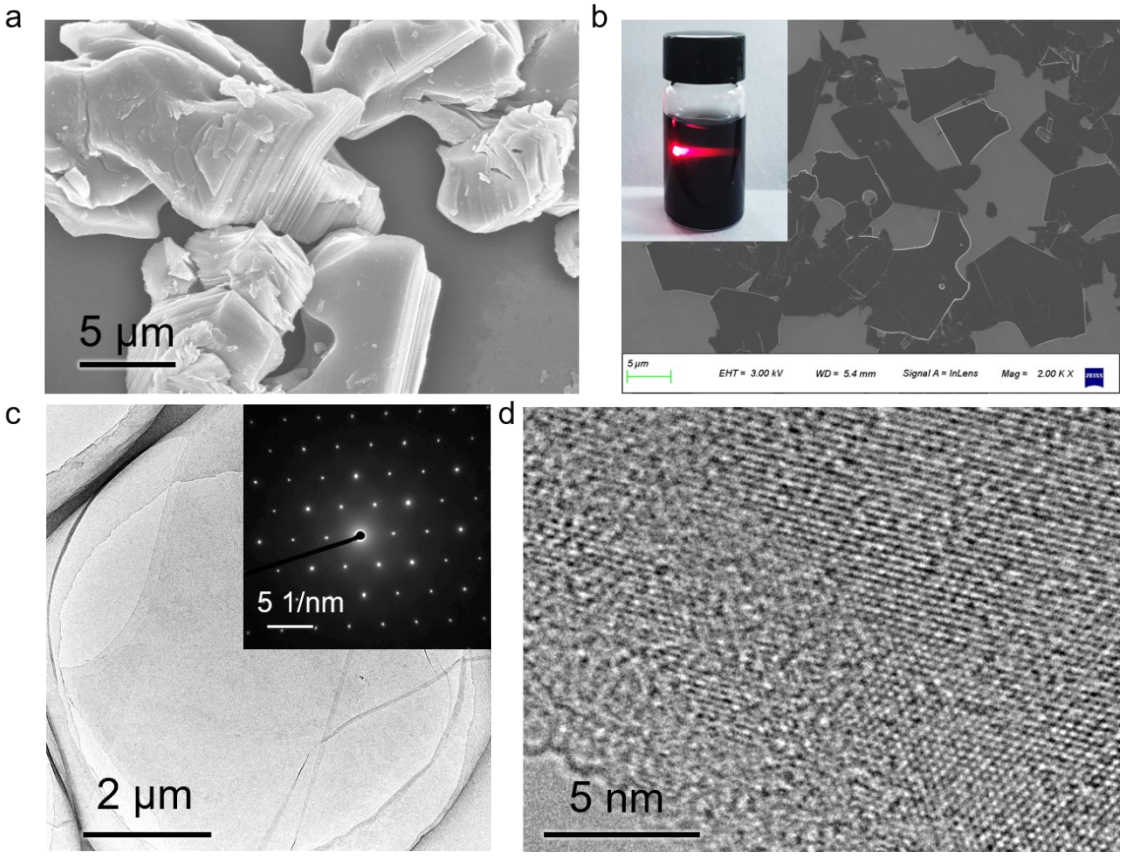

Figure S3. (a**)** SEM image of Ti_3AlC_2 powder showing the compact layered structure. (b) SEM image of $Ti_3C_2T_X$ nanosheets and inserted optical image of the MXene aqueous dispersion showing a typical Tyndall scattering effect. (c) TEM image and inserted electron diffraction of single-layer $Ti_3C_2T_X$. (d) HRTEM image of MXene nanosheets.

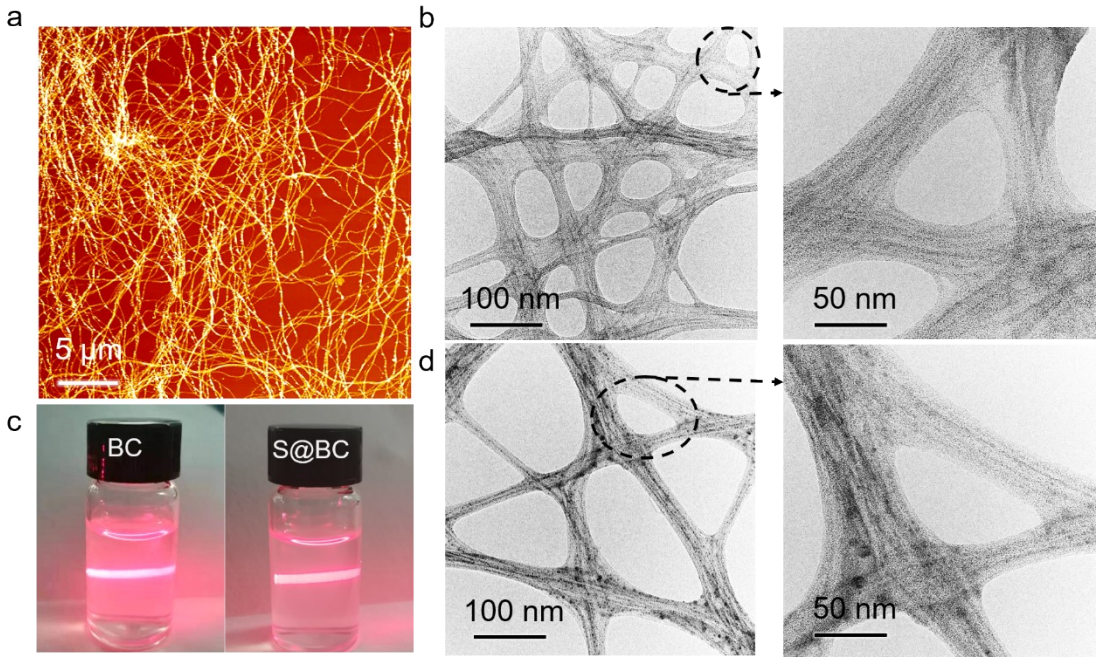

Figure S4. Morphologies of BC and Silyated BC. (a) AFM image of BC showing a quite high aspect ratio. (b) TEM images of BC networks. (c) Stable colloidal suspension of BC and silylated BC. (d) TEM images of silylated BC networks.

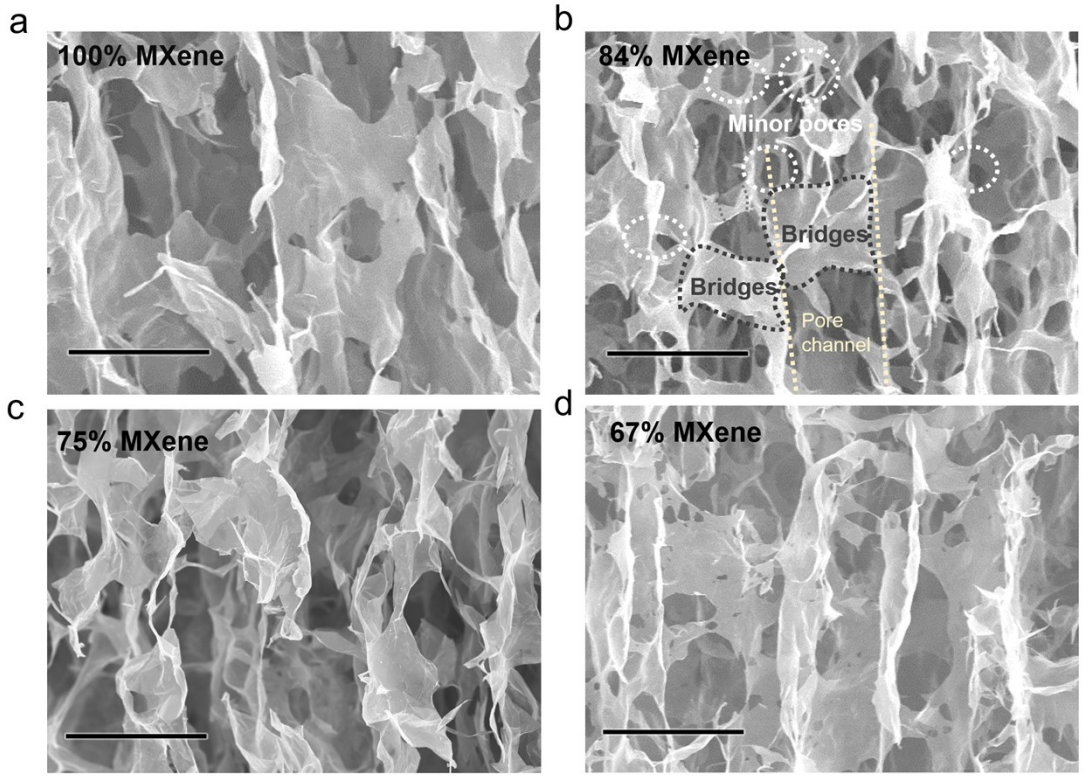

Figure S5. Cross-sectional SEM images of (a) pure MXene aerogel and (b-d) S@BC-MX84%, S@BC-MX75%, and S@BC-MX67% aerogels. Scale bar is 50 μm and applies to all images.

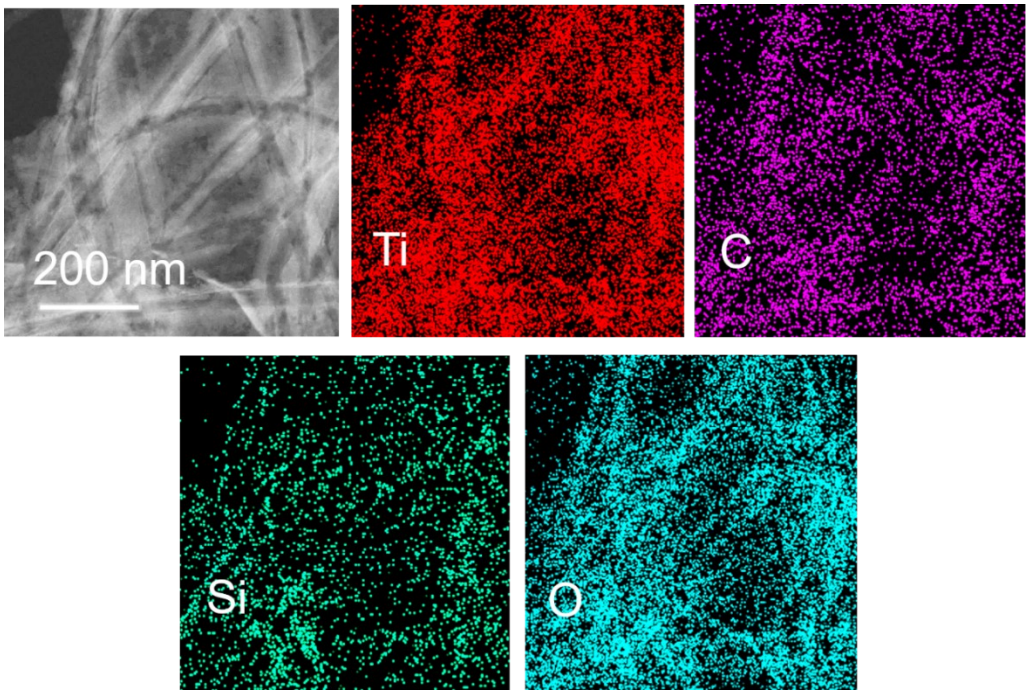

Figure S6. HADDF-STEM image of S@BC-MX50% aerogel and corresponding EDS mapping images of Ti, C, Si, and O.

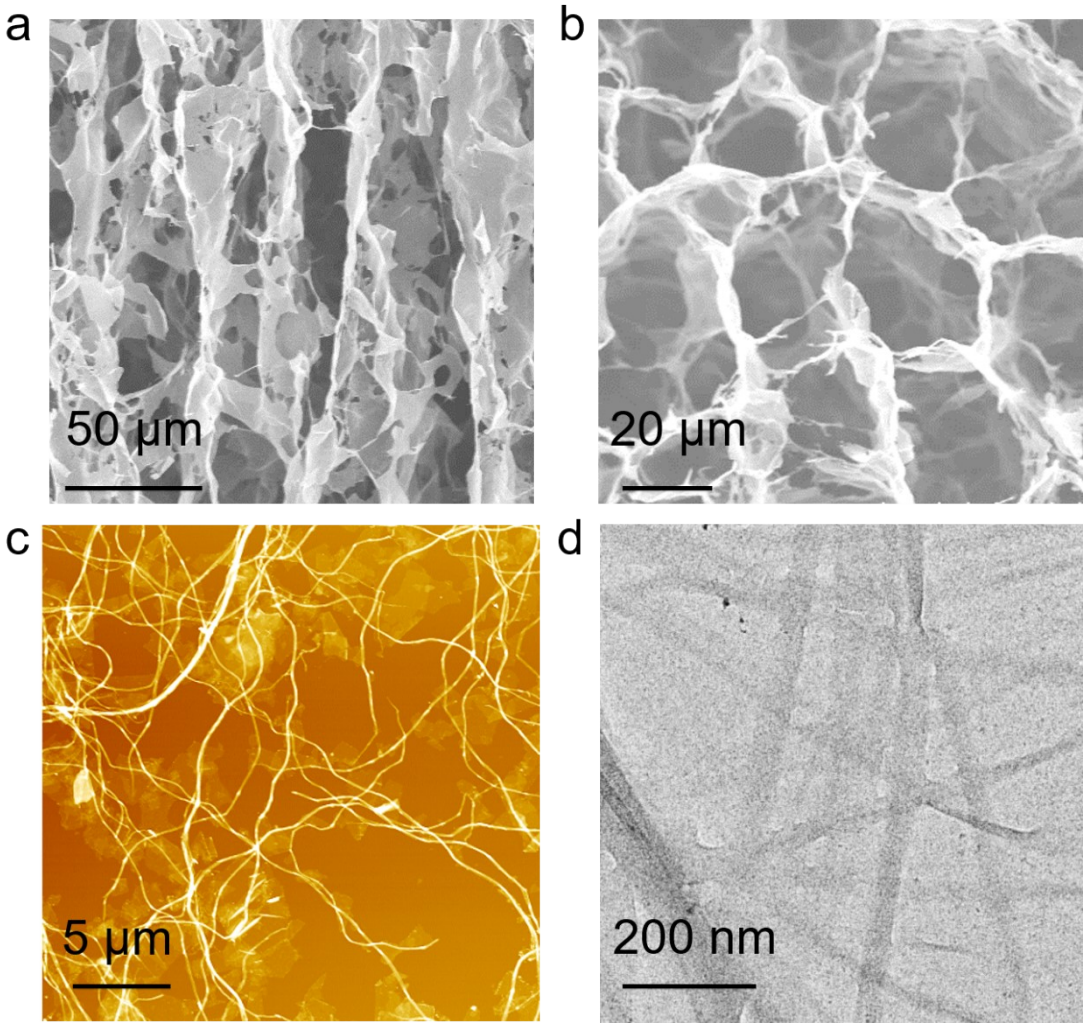

Figure S7 Morphologies of BC-MX50% hybrid aerogel. (a) cross-sectional SEM image. (b) Top-view SEM image. (c) AFM image of MXene nanosheets assembled with BC nanofibers. (d) TEM image of cell wall.

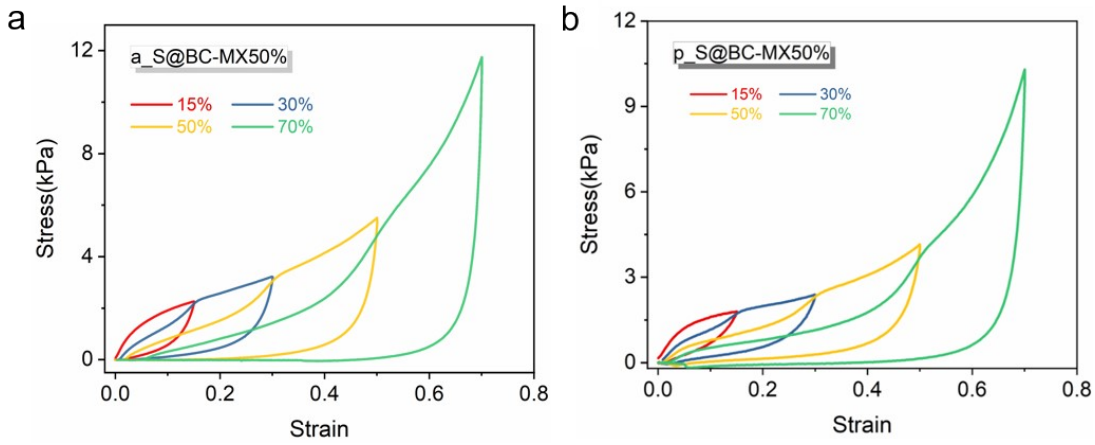

Figure S8. Stress-strain curves of S@BC-MX50% aerogel compressed along (a) "a" and (b) "p_" directions.

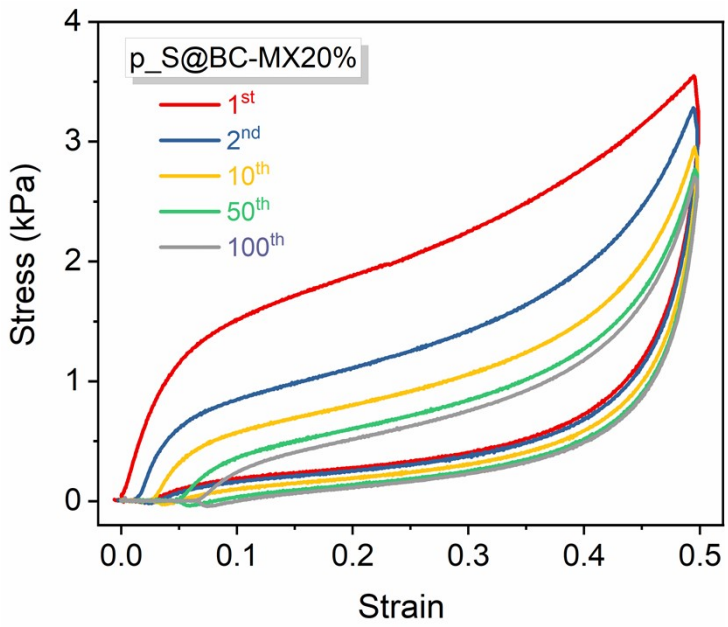

Figure S9. Stress-strain curves of S@BC-MX20% aerogel along "p_" direction at 50% strain for 100 cycles.

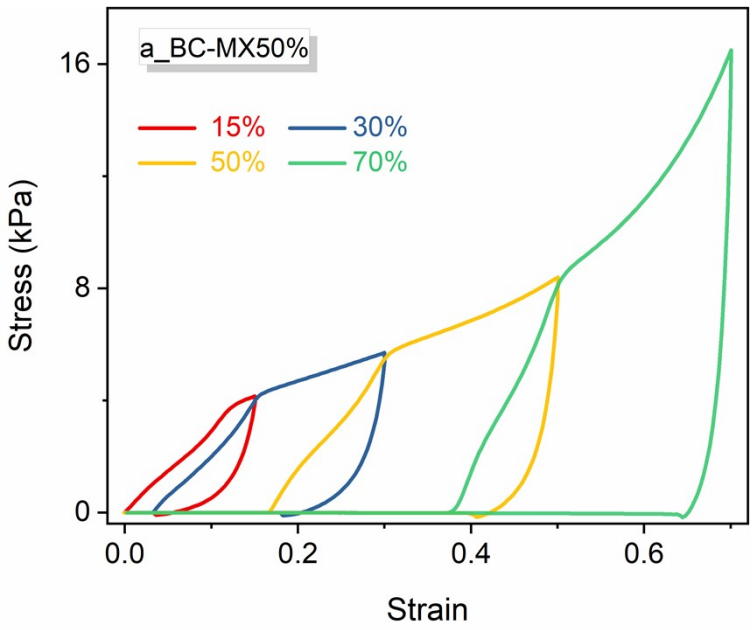

Figure S10. Stress-strain curves of unmodified BC-MX50% aerogel compressed at "a_" direction.

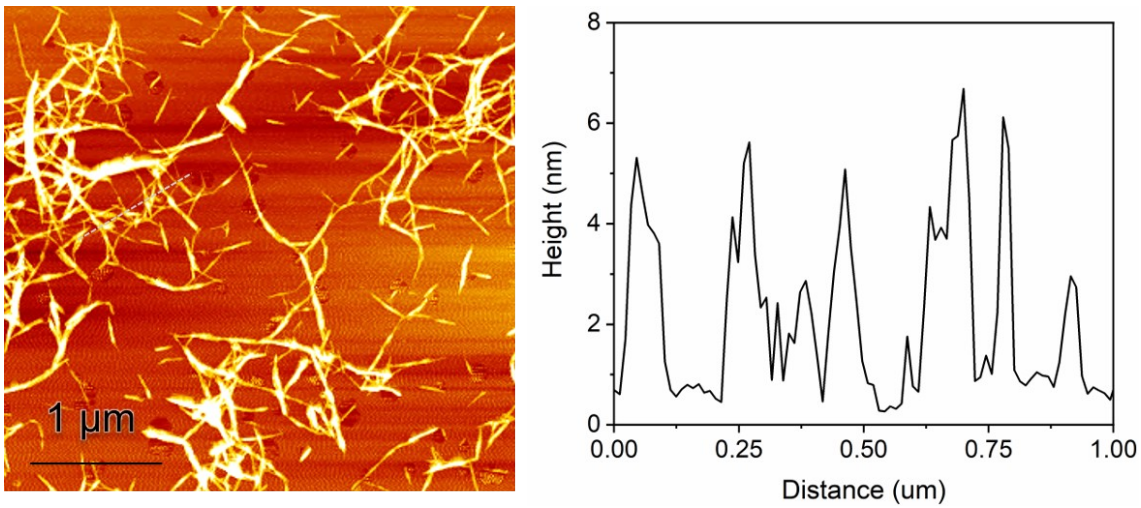

Figure S11. AFM image and height profile of CNF.

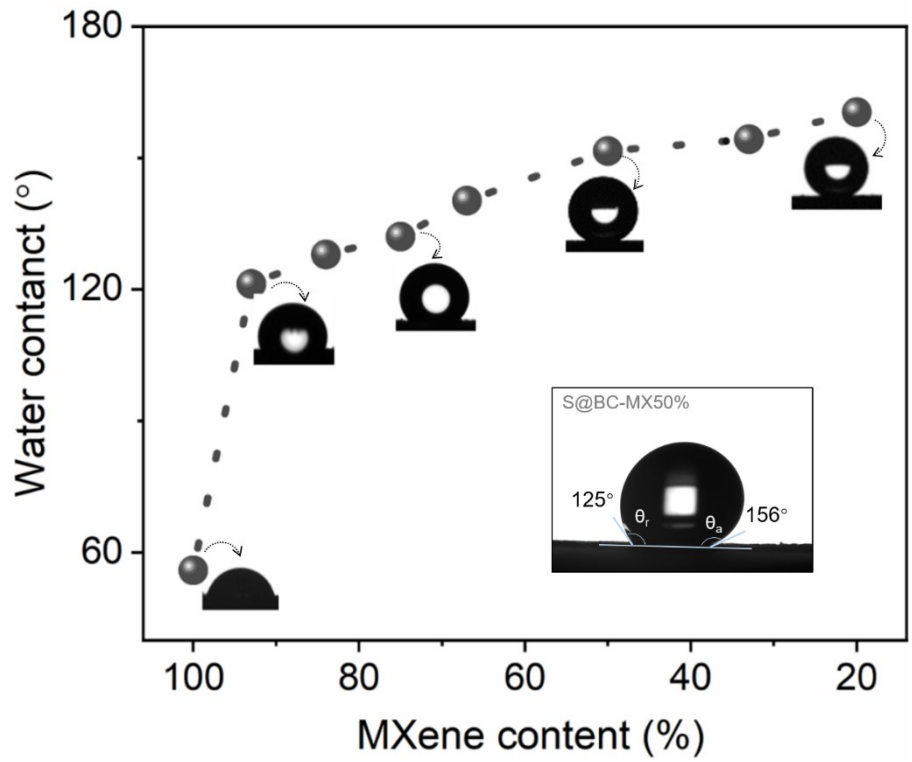

Figure S12. Water contact angle of S@BC-MX aerogels with different MXene contents, with the bottom right inset showing the advancing and receding contact angles of S@BC-MX50% aerogel measured by tilted plate experiments.

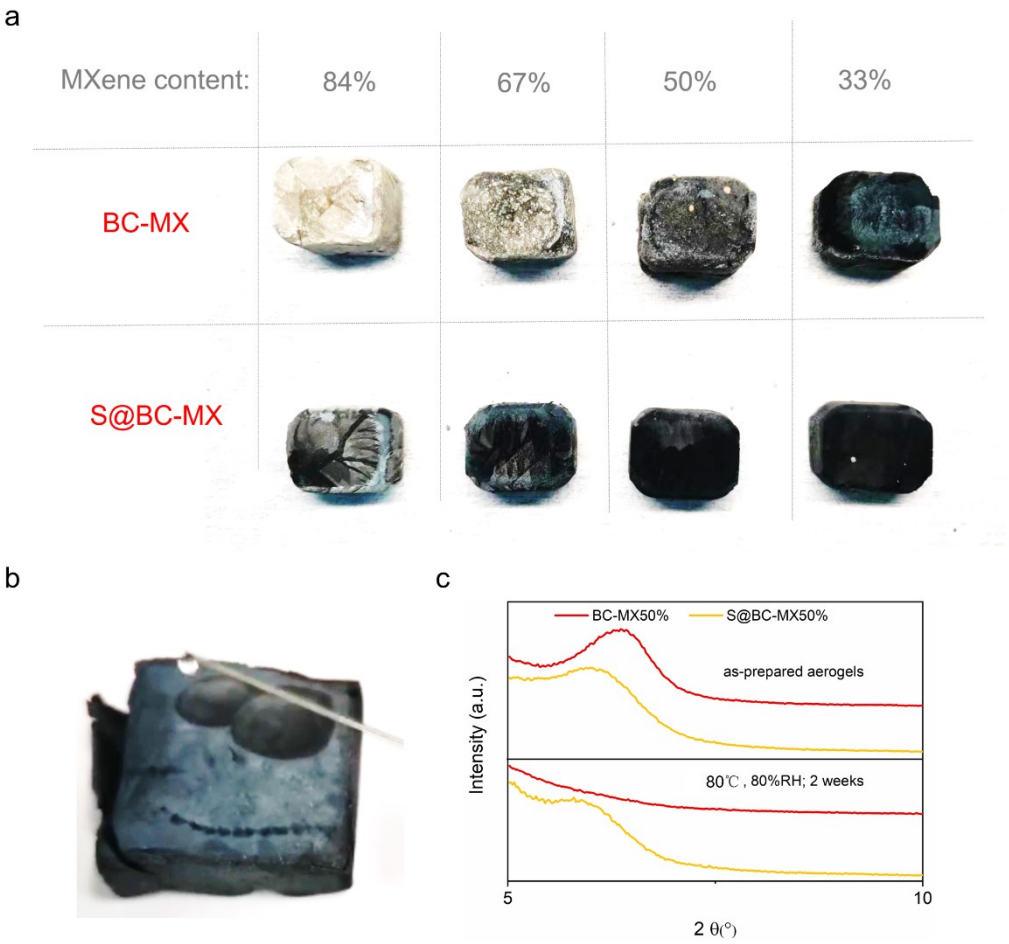

Figure S13. (a) The real-object pictures of BC-MX aerogels and S@BC-MX aerogels after being exposed to humid air for 2 weeks at 80°C under a constant relative humidity of 80%. (b) The structural collapse of unmodified BC-MX50% aerogel touched with water droplets. (c) XRD patterns of BC-MX50% aerogels and S@BC-MX50% aerogels before and after aging tests in humid air.

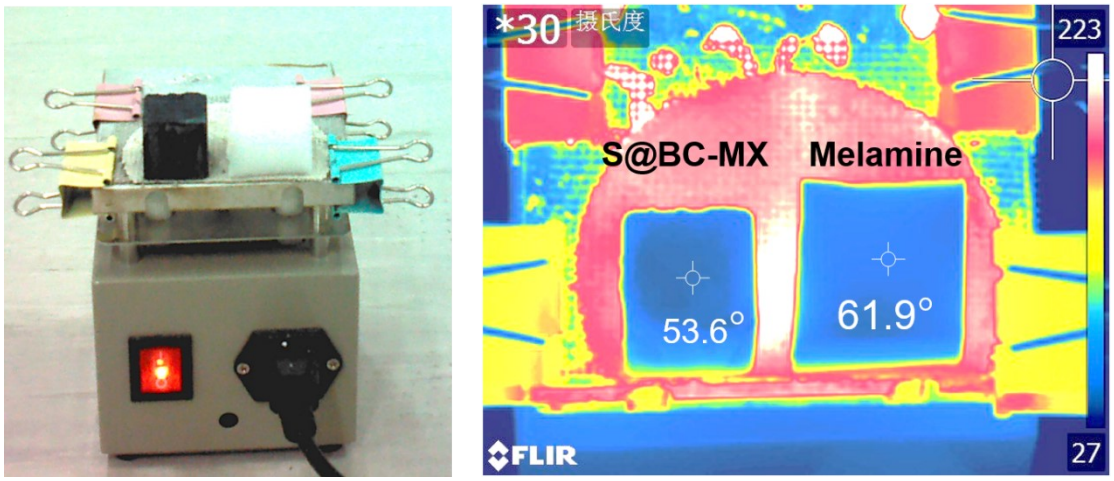

Figure S14. Physical and thermographic images of S@BC-MX50% aerogel and melamine foam (density: 9.1mg/cm^3, thickness: 25mm) on a heating plate of ~235 °C.

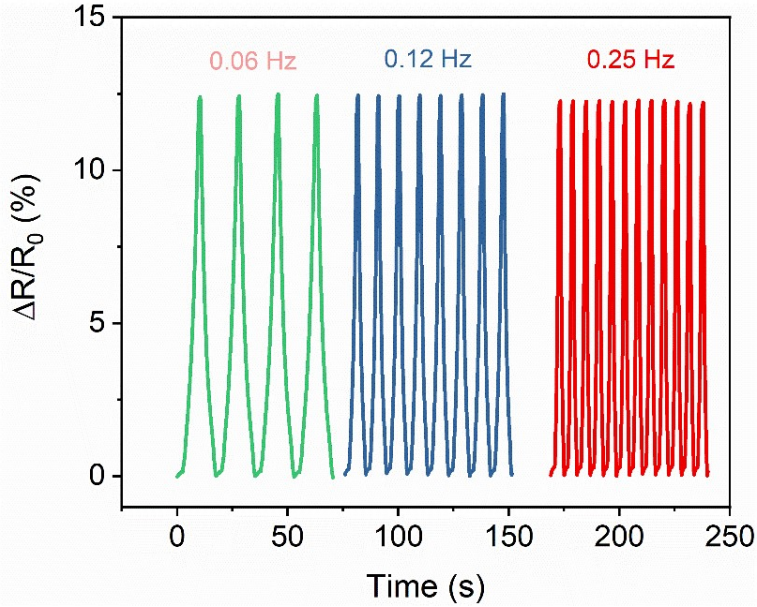

Figure S15. Normalized resistance changes of the S@BC-MX67% aerogel at 30% strain with different deformation frequencies.

Table S1. Comparison of hydrophobicity, electrical conductivity and compression property of nanocellulose- and MXene- based elastic aerogel materials.

Materials	Density (mg/cm^3)	Water contact angle (°)	Electrical conductivity (S/m)	Compression properties				Ref.
				Strain (%)	Cycle	Height retention (%)	Stress retention (%)	
S@BC-MX50%	**6.2**	**152**	**7**	**50**	**500**	**85**	**60**	**This work**
S@BC-MX84%	**6.2**	**128**	**118**	**50**	**100**	**87.5**	**61**	
Pure MXene	11.0	Hydrophilic	-	50	20	84	95	1
Silylated CNF	17.3	138	Insulating	50	1	96	-	2
Silylated PVA/CNF	10.2	142	Insulating	70	100	82	86	3
MXene/CNF/PU	-	152	-	40	100	82	76	4
MXene/ANF	25.0	Hydrophilic	-	30	1000	96	92	5
MXene/CNT	9.1	Hydrophilic	447	50	100	93	79	6
Carbonized BC/MXene	26.2	Hydrophob-ic	0.013	50	5000	98	91	7
MXene/GO	12.2	99	31.6	50	100	99	93	8
MXene/PI	13.8	-	0.4	50	1000	86	90	9

Table S2. Elemental content of S@BC-MX aerogels with different concentrations of MXene.

MXene content	Ti（at%）	C（at%）	Si（at%）	O（at%）	F（at%）	Cl（at%）
100%	38.1	28.0	-	21.2	11.5	1.2
93%	27.6	31.7	1.0	26.4	11.5	1.8
84%	25.1	27.5	2.1	34.1	9.3	1.9
75%	17.6	38.6	2.8	34.1	5.4	1.5
67%	14.5	39.9	3.8	34.4	5.9	1.5
50%	9.1	37.0	5.1	41.2	6.7	0.9
33%	5.0	42.0	9.0	39.7	3.7	0.6

Table S3. Comparison of the absorbent capacity of various hydrophobic aerogel materials towards organic solvents and oils.

Absorbent materials	Density (mg/cm^3)	Water contact angle	Absorbent capacity (g/g)	Ref.
Silylated BC/MXene	**6.2**	**152**	**88-210**	**This work**
Silyated cellulose	2.9-16.6	142	51-143	10
Methyltrichlorosilane modified PVA-CNF	13	150	44-96	11
Trimethylsilylation modified bacterial cellulose	6.7	147	80-185	12
Carbonaceous fiber from raw cotton	12	120	55-183	13
Carbonaceous fiber from bacterial cellulose	4-6	129	106-321	14
CNT	5-10	156	87-176	15
Graphene-CNT	2.1-4.3	92-140	125-533	16
GO	4.4-7.9	155	100-250	17
APTES-modified GO-GO nanoribbon	2.3-4.1	142	98-447	18
GO-GO nanoribbon	2.2-6.8	-	100-350	19

Table S4. Electrical conductivities of S@BC-MX aerogels and BC-MX aerogels with various MXene contents at the density of 6.2 mg/cm^3.

MXene content (wt%)	Electrical conductivity of S@BC-MX aerogels (S/m)	Electrical conductivities of BC-MX aerogels(S/m)
100	163	163
93	132.1	118.5
84	117.6	108.4
75	61.6	48.8
67	38.9	33.7
50	7.8	7.0
33	0.07	1.3

References

1. M. Han, X. Yin, K. Hantanasirisakul, X. Li, A. Iqbal, C. B. Hatter, B. Anasori, C. M. Koo, T. Torita and Y. Soda, *Advanced Optical Materials*, 2019, **7**, 1900267.
2. Z. Zhang, G. Sèbe, D. Rentsch, T. Zimmermann and P. Tingaut, *Chemistry of Materials*, 2014, **26**, 2659-2668.
3. X. Zhang, H. Wang, Z. Cai, N. Yan, M. Liu and Y. Yu, *ACS Sustainable Chemistry & Engineering*, 2018, **7**, 332-340.
4. C. Cai, Z. Wei, Y. Huang and Y. Fu, *Chemical Engineering Journal*, 2021, **421**, 127772.
5. L. Wang, M. Zhang, B. Yang, J. Tan and X. Ding, *ACS Nano*, 2020, **14**, 10633-10647.
6. Z. Deng, P. Tang, X. Wu, H.-B. Zhang and Z.-Z. Yu, *ACS Applied Materials & Interfaces*, 2021, **13**, 20539-20547.
7. Z. Chen, Y. Hu, H. Zhuo, L. Liu, S. Jing, L. Zhong, X. Peng and R.-c. Sun, *Chemistry of Materials*, 2019, **31**, 3301-3312.
8. D. Jiang, J. Zhang, S. Qin, Z. Wang, K. A. S. Usman, D. Hegh, J. Liu, W. Lei and J. M. Razal, *ACS Nano*, 2021, **15**, 5000-5010.
9. J. Liu, H. B. Zhang, X. Xie, R. Yang, Z. Liu, Y. Liu and Z. Z. Yu, *Small*, 2018, **14**, 1802479.
10. O. Laitinen, T. Suopajärvi, M. Österberg and H. Liimatainen, ACS applied materials & interfaces, 2017, 9, 25029-25037.
11. Q. Zheng, Z. Cai and S. Gong, Journal of materials chemistry A, 2014, 2, 3110-3118.
12. H. Sai, R. Fu, L. Xing, J. Xiang, Z. Li, F. Li and T. Zhang, ACS applied materials & interfaces, 2015, 7, 7373-7381.
13. H. Bi, Z. Yin, X. Cao, X. Xie, C. Tan, X. Huang, B. Chen, F. Chen, Q. Yang and X. Bu, Advanced Materials, 2013, 25, 5916-5921.

14. Z. Y. Wu, C. Li, H. W. Liang, J. F. Chen and S. H. Yu, Angewandte Chemie, 2013, 125, 2997-3001.
15. X. Gui, J. Wei, K. Wang, A. Cao, H. Zhu, Y. Jia, Q. Shu and D. Wu, Advanced materials, 2010, 22, 617-621.
16. W. Zhan, S. Yu, L. Gao, F. Wang, X. Fu, G. Sui and X. Yang, ACS applied materials & interfaces, 2018, 10, 1093-1103.
17. J. Li, J. Li, H. Meng, S. Xie, B. Zhang, L. Li, H. Ma, J. Zhang and M. Yu, Journal of Materials Chemistry A, 2014, 2, 2934-2941.
18. S. Hou, X. Wu, Y. Lv, W. Jia, J. Guo, L. Wang, F. Tong and D. Jia, Applied Surface Science, 2020, 509, 144818.
19. C. Wang, X. He, Y. Shang, Q. Peng, Y. Qin, E. Shi, Y. Yang, S. Wu, W. Xu and S. Du, Journal of Materials Chemistry A, 2014, 2, 14994-15000.